

. . . 1, . . . I 1, . . . 1, . . . 2

1

. . . , 15, 49005, . . . ; e-mail: nikolaev.o.d@nas.gov.ua

2

, 72, 49000, . . .

( . . . )

( 1000 )

3D

)»

«

(

2D

( . . . 2,5

56 ).

Dynamic processes in the combustion chamber have a significant effect on the characteristics of the working processes of solid-propellant rocket engines (SPREs). Pressure jumps and a sharp increase in the local temperature of the combustion products in non-stationary engine operation modes can lead to overrating values of operating parameters and a failure of the SPRE combustion chamber structure. The dynamic processes in the SPRE combustion chamber develop in a complex interconnection of a large number of physical and chemical processes that occur in the gas-dynamic part of the working space of the engine chamber and often lead to self-oscillating modes of engine operation. This is evidenced by numerous data on SPRE fire tests. This paper presents the results of a numerical study of the effect of the SPRE chamber inner surface roughness on SPRE operating parameter low-frequency self-oscillations. The study was made using up-to-date computer simulation means and analysis.

Low-frequency (up to 1,000 Hz) oscillations in an SPRE combustion chamber were studied for a power plant test chamber in cold operation with the use of two different approaches to numerical modeling of the dynamics of in-chamber processes: the development and study of a 3D model of the dynamic system of combustion chamber structure – combustion products using the finite element method and the development and study of an axisymmetric 2D model of engine chamber gas flow using the finite volume method.

The study revealed a self-oscillatory flow regime caused by combustion product vorticity and acoustic feedback due to vortices colliding with the chamber components or the SPRE nozzle. It was shown that accounting for the wall roughness increased gas vorticity in the gas–solid dynamic interaction zone and the chamber gas oscillation amplitude (on the average, by a factor of 2.5 at a maximum wall roughness height of 56 μm). The calculated gas flow pattern in the vorticity zones of the chamber and the low-frequency gas pressure oscillation parameters are in qualitative agreement with the experimental ones.

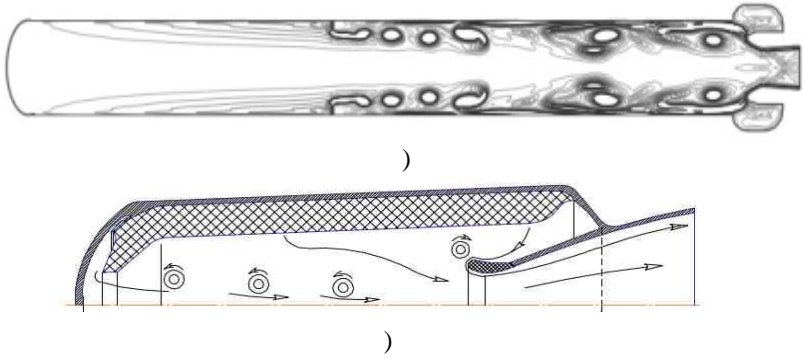
**Keywords:** solid propellant rocket engine, working process self-oscillations, combustion product flow vorticity, acoustic oscillations, chamber wall surface roughness, finite volume method.



[10] – [14]).

Titan-IV SRMU ( ), Space Shuttle RSRM, Titan-34D SRM, Ariane 5 ( ), -300 ( ) [3], [15], [16], [17]. (P230 motor) Ariane 5 [3],

-300 [17].



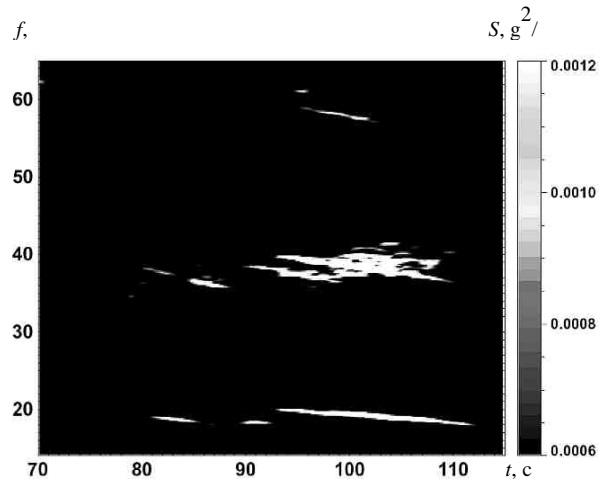
. 1 –

Ariane 5 ( ) -300 ( )

IV [16].

.2

IV 90 < t < 112 c  
14 50



. 2 – Waterfall-

Titan-IV SRMU

[16]

[6], [9], [17],

$$L/d \geq 4, (L \ d -$$

2000 ( [18]

0.3 5 ).

100 (

VKI

[19]

1000 )

«

–

» (

ANSYS Mechanical [19].

(3D)

[20].

Method)

FLUENT [19],

(2D )  
(FVM-Finite Volume  
LES  
FLUENT  
[19]

LES

( ., [21]).

(LES);

2.

2.1

(LES)

FLUENT.

$$\frac{\partial \bar{\rho}}{\partial t} + \frac{\partial \bar{\rho} \tilde{u}_i}{\partial x_i} = 0, \quad (1)$$

$$\frac{\partial}{\partial t}(\bar{\rho} \tilde{u}_i) + \frac{\partial}{\partial x_i}(\bar{\rho} \tilde{u}_i \tilde{u}_j) = -\frac{\partial \bar{p}}{\partial x_i} + \frac{\partial}{\partial x_i}(\tilde{\sigma}_{ij} - \tau_{ij}^{xyz}), \quad (2)$$

$$\frac{\partial}{\partial t}(\bar{\rho} \tilde{e}) + \frac{\partial}{\partial x_i}(\bar{\rho} \tilde{u}_i \tilde{e}) = \frac{\partial}{\partial x_i}(-\bar{p} \tilde{u}_i - \bar{q}_i + \tilde{u}_i \tilde{\sigma}_{ij} - H_i^{xyz} - \Theta_i^{xyz}), \quad (3)$$

 $\bar{\rho}, \bar{u}$ ;  $\tilde{u}$ :  $\tilde{u} = \overline{\rho u} / \bar{\rho}, e(x, t)$  $t$  $x; p$ ;  $\tilde{\sigma}_{ij}$  $\bar{q}_i$ 

$$\tilde{\sigma}_{ij} = \mu \left( \frac{\partial \tilde{u}_i}{\partial x_j} + \frac{\partial \tilde{u}_j}{\partial x_i} \right) - \frac{2}{3} \mu \frac{\partial \tilde{u}_k}{\partial x_k} \delta_{ij}, \quad (4)$$

$$\bar{q}_i = -\bar{K} \frac{\partial \bar{T}}{\partial x_i}, \quad (5)$$

 $H_i^{sgs}, \Theta_i^{sgs}$ 

$$H_i^{sgs} = \frac{-\mu_t}{P_r} \frac{\partial H_i}{\partial x_i}, \quad (6)$$

$$\Theta_i^{sgs} = C_\varepsilon \bar{\rho} (k_{sgs})^{3/2} / V^{1/3}, \quad (7)$$

 $C_I, C_\varepsilon$  $P_r$ :  $C_I = 0,0066; C_\dagger = 1,1; P_r = 0,85; \tau_{ij}^{sgs}$ 

(SGS):

$$\tau_{ij}^{sgs} = -2\mu_i (\tilde{S}_{ij} - \tilde{S}_{kk} \delta_{ij} / 3) + 2(\bar{\rho} k^{sgs} \delta_{ij}) / 3, \quad (8)$$

 $\tilde{S}_{ij}$ 

:

$$\tilde{S}_{ij} = \frac{1}{2} \left( \frac{\partial \tilde{u}_i}{\partial x_j} + \frac{\partial \tilde{u}_j}{\partial x_i} \right). \quad (9)$$

$$\mu_t = \rho C_w^2 V^2 \tilde{S}_{ij}^d \quad (6)$$

$$\mu_t = \bar{\rho} C_w^2 V^{2/3} \frac{(S_{ij}^d S_{ij}^d)^{3/2}}{(\bar{S}_{ij} \bar{S}_{ij})^{5/2} + (\bar{S}_{ij}^d \bar{S}_{ij}^d)^{5/4}}, \quad (10)$$

$$V = \sqrt{\frac{2}{\rho} \tilde{S}_{ij}^d};$$

$$S_{ij}^d = \frac{1}{2} \left( \frac{\partial \tilde{u}_i}{\partial x_k} \frac{\partial \tilde{u}_k}{\partial x_j} + \frac{\partial \tilde{u}_j}{\partial x_k} \frac{\partial \tilde{u}_k}{\partial x_i} \right) - \frac{1}{3} \frac{\partial \tilde{u}_k}{\partial x_k} \frac{\partial \tilde{u}_k}{\partial x_k} \delta_{ij}.$$

FLUENT WALE  $C_w = 0,325$  [19].

$$k_{sgs} = C_I V^{2/3} \tilde{S}_{ij} \tilde{S}_{ij} \quad (7)$$

$$k_{sgs} = C_I V^{2/3} \tilde{S}_{ij} \tilde{S}_{ij} \quad (11)$$

$$p = \rho RT, \quad (12)$$

$p$  – тиск,  $\rho$  – густина,  $T$  – температура,  $R$  – газова стала:  $R = 8,314 \text{ Дж/(кг} \cdot \text{К)}$ .

Artificial Compressibility

FLUENT.

$1 \times 10^{-6}$  (1) – (12), 0.33

## 2.2

1/30

VKI (1/30) Ariane 5 (P230 motor), [18],



. 3 –

[18]

0.038 .  
 0.029 ,  
 Ariane 5),

$r_0$  0.015 ,  
 $R$ ,

( 0.19

1, 2 3.

1 [18].

1 -

VKI

	1.4
$C_p, / \times$	1006.43
$\sim, / *$	$1.7894 \times 10^{-5}$
$M, /$	28.966

« [19], »

VKI

VKI  
 FLUENT LES [19]  
 2D

VKI

2D ( ( 1) - 82273 , ( )  
 ( 2) - 35000 ).

2

( 1),  
 VKI - « ( 2), »

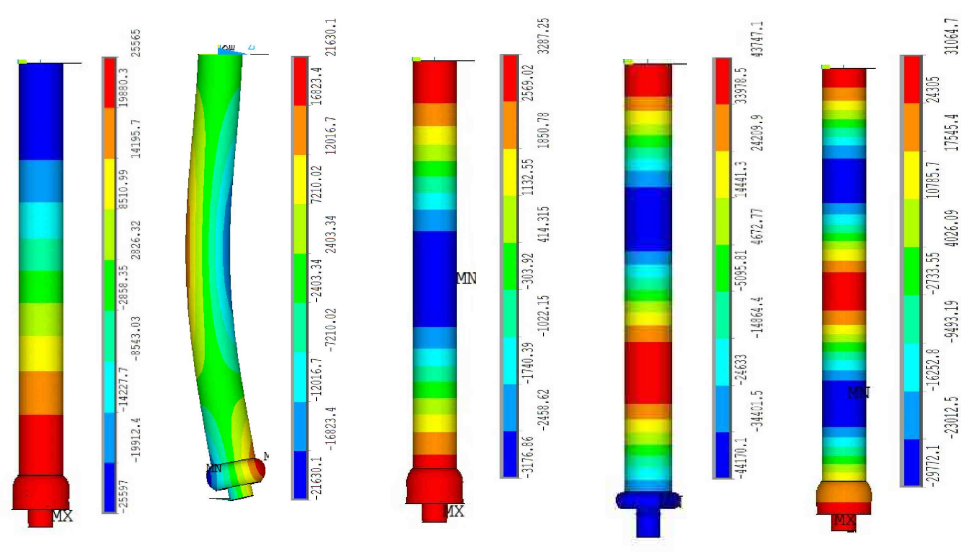
VKI - ( 4). 3-  
 «



VKI – «L», T –  
 : L, T –  
 L+T –  
 2 – VKI,  
 « VKI – » VKI-

1	2	3	4
280	219	1L	183
–	–	–	304
–	439	2L	428
464	466	2L+1T	500
685	664	3L	619
925	893	4L	887

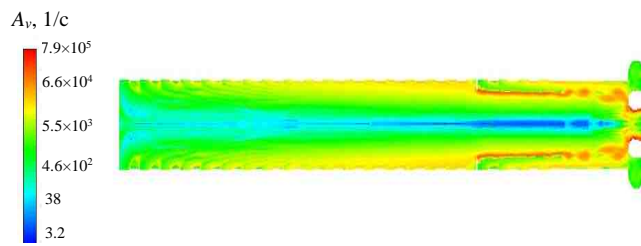
, 2,  
 ,  
 .4  
 ( $P_{ch}$ , [ ]) VKI ( 1)  
 « VKI – ».



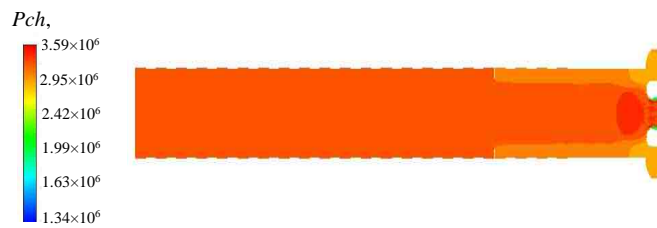
) ) ) ) ) )  
 ), ), ), ) – 219 , 439 , 664 ,  
 894 ; ) – 466  
 .4 – VKI ( 1)

, .4, ), 4, ), 4, ), 4, )  
 1L, 2L, 3L, 4L 219 , 439 , 664 , 894 ( )  
 ), .4, ) -  
 466 . ,  
 , ,  
 . VKI,  
 ( .5 - 8)

. .5 - 6 VKI  
 $A_v (A_v - P_{ch})$   
 $t = 0.33c.$

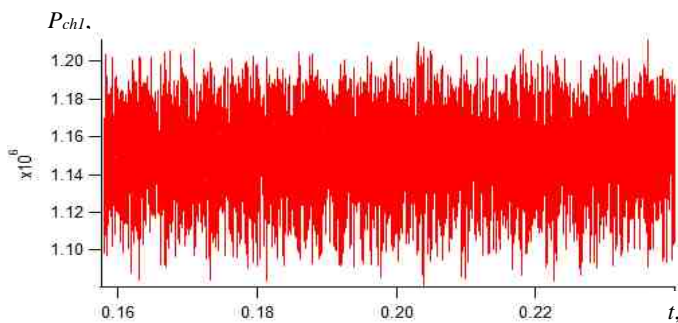


.5 - VKI



.6 - VKI

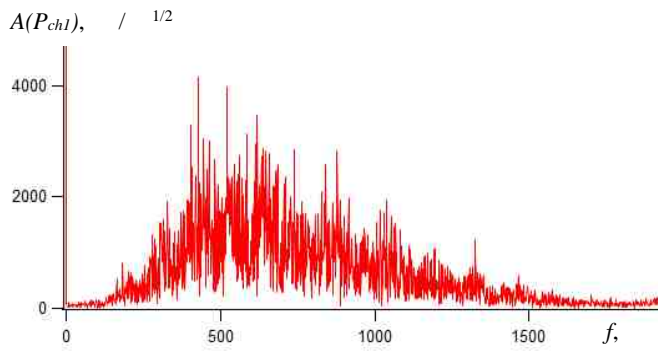
.7  $P_{chl}(t)$   $P_{ch}$  VKI 1,  
 , 1  
 1 .



.7 -  $P_{ch}$  VKI 1

.8  
 1 VKI  $P_{chl}$  (  
 304 ,428 ,500 ,619 ,887 ).

183 ,



.8 -

VKI 1

.8,

400 600

500 ( .4, ))

VKI ( 2)

VKI -

( 1),

466 ( . 2,

2,4).

3.

2D

VKI ( 2)

VKI

.3.

56

.9 - 12

VKI

( .9)

( .10)

$t = 0.33c;$

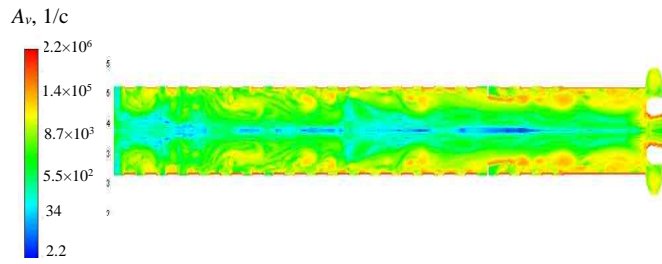
$t$  1,

( .11);

1 ( .12).

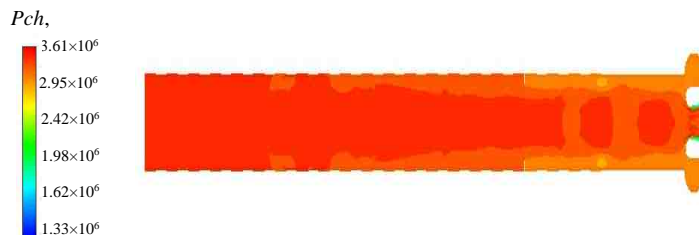
VKI

.5 - 9.



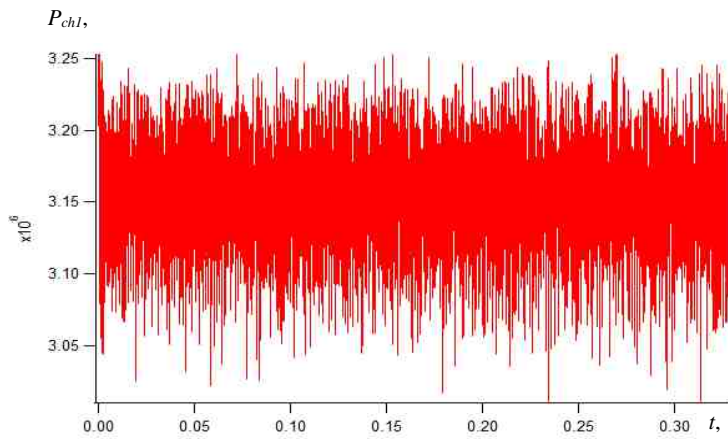
. 9 –

VKI,



. 10 –

VKI,



. 11 –

VKI

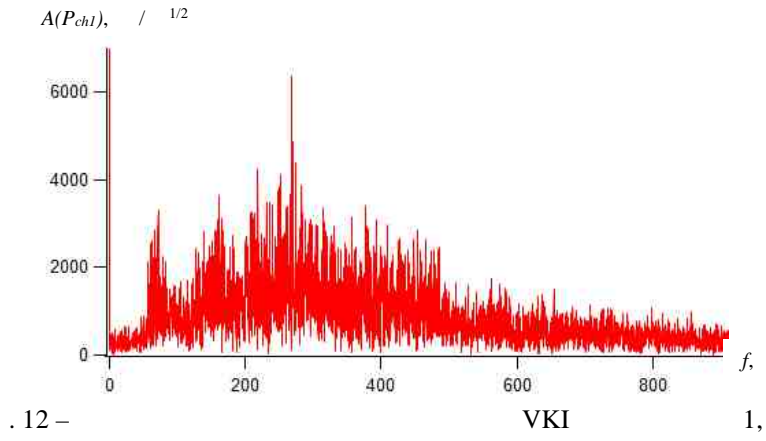
1,

. 7, 11

2.5

. 6, 10).

( . 12).  
VKI



1000 10 : 72 , 161 , 219 , 268 ,  
 377 , 454 , 563 , 654 , 798 , 856 .

2, , -  
 1000 , 6  
 10. - 72  
 161 , ,

72 , 161 , -  
 , -

1. ( 1000 ) -  
 -  
 -

« - 3D ( -  
 )» , , -

2D , .  
 , .

2. ( ) 1/30  
 - Ariane 5 -  
 VKI, Karman Institute for Fluid Dynamics ( ) -  
 VKI  
 ' - (2D) -  
 ;  
 (LES);  
 ( ) -  
 ,  
 .  
 VKI. , -  
 , ( ) -  
 , .  
 VKI. ,  
 3. VKI, ,  
 1000 , -  
 , -  
 , ,  
 4. 2D , .  
 ( , -  
 56 ), -  
 2.5 . ( ) -  
 , -  
 1000 6 10, -  
 (72 161 ), -  
 , -  
 , -  
 ,  
 .

1. Glazunov A. A., Eremin I. V., Zhiltsov K. N., Kostyushin K. V., Tyryshkin I. M., Shuvarikov V. A. Numerical investigation of the pressure pulsation magnitude and natural aeroacoustic frequencies in the combustion chambers with a charge of a complex shape. Vestnik Tomskogo gosudarstvennogo universiteta. Matematika i mekhanika. 2018. No 53. P. 59–72. [https://doi: 10.17223/19988621/53/6](https://doi.org/10.17223/19988621/53/6)
2. Fabignon Y., Dupays J., Avalon G., Vuillot F., Lupoglazoff N., Casalis G., Prévost M. Instabilities and pressure oscillations in solid rocket motors. Aerospace Science and Technology. 2003. No 7. P. 191–200. [https://doi: 10.1016/S1270-9638\(02\)01194-X](https://doi.org/10.1016/S1270-9638(02)01194-X)
3. Zeldovich J. B. Selected Works. Chemical Physics and Hydrodynamics. Moscow: Nauka, 1984. 374 p.
4. Culick F. E.; Kuentzmann P. Unsteady Motions in Combustion Chambers for Propulsion Systems. NATO Research and Technology Organization Neuilly-Sur-Seine: Paris, France, 2006. 664 p.
5. Yash Pal, Ravi Kumar V. Physical and Ballistic Characterization of Aluminum-Loaded Paraffin Hybrid Rocket Fuels. Energy & Fuels. American Chemical Society. 2017. 31(9). P. 10133–10143. [https://doi: 10.1021/acs.energyfuels.7b01636](https://doi.org/10.1021/acs.energyfuels.7b01636)
6. Ganesan S., Chakravarthy S. R. Effect of Acoustic Pressure Oscillations on Burning Rate Augmentation of Composite Solid Propellants at Different Initial Grain Temperatures. Combustion Science and Technology. 2023. <https://doi.org/10.1080/00102202.2023.2248369>
7. Taherinezhad R., Zarepour G. Theoretical, Numerical and Experimental Investigation of Vortex Shedding in a Novel Sub-Scaled Motor. Journal of Applied Fluid Mechanics. 2019. Vol. 12, No. 4. P. 1319–1332.
8. Bhutto A. A., Harijan K., Hussain M., Shah S. F., Kumar L. Numerical Simulation of Transient Combustion and the Acoustic Environment of Obstacle Vortex-Driven Flow. Energies. 2022. 15(16) 6079. 11 p. <https://doi.org/10.3390/en15166079>
9. Sanjeev Malhotra. On Combustion Instability in Solid Rocket Motors. Thesis of the dissertation for the degree of Doctor of Philosophy. California Institute of Technology Pasadena, California. 2004. 122 p. URL: <https://thesis.library.caltech.edu/1648/1/thesis.pdf>
10. Ferretti V., Favini B., Cavallini E., Serraglia F., Giacinto M. D. Pressure oscillations simulation in P80 SRM first stage VEGA launcher. San Diego. American Institute of Aeronautics and Astronautics. 2011. P. 102–116.
11. Dotson W., Sako B. H. Interaction Between Solid Rocket Motor Internal Flow and Structure During Flight Kirk Journal of Propulsion and Power. 2007. January–February. Vol. 23, No. 1. P. 140–145. [https://doi:10.2514/1.20477](https://doi.org/10.2514/1.20477)
12. Zhang Q., Wang N., Li J., Su W., Zhang Y. Effect of the head cavity on pressure oscillation suppression characteristics in large solid rocket motors. Science China. Technological Sciences. 2015. July. Vol. 58, No. 7. P. 1250–1262. [https://doi: 10.1007/s11431-015-5834-z](https://doi.org/10.1007/s11431-015-5834-z)
13. Kohnke P. Ansys Inc. Ansys Manual. 001369. Twelfth Edition. Canonsburg : SAS IP, 2001. 1266 p.
14. Nikolayev O. D., Bashliy I. D. Assessment of thrust chamber stability margins to high-frequency oscillations based on mathematic modeling of coupled ‘injector - rocket combustion chamber’ dynamic system. Technical mechanics. 2022. No 1. P. 3–17. <https://doi.org/10.15407/itm2022.01.003>
15. Qin W. J., Xie M. Z., Jia M., et al. Large eddy simulation and proper orthogonal decomposition analysis of turbulent flows in a direct injection spark ignition engine: Cyclic variation and effect of valve lift. Science China Technological Sciences. 2014. 57(3). P. 489–504. [https://doi:10.1007/s11431-014-5472-x](https://doi.org/10.1007/s11431-014-5472-x)
16. Nicoud F., Ducros F. Subgrid-scale stress modeling based on the square of the velocity gradient tensor. Flow Turbulence and Combustion. 1999. 62(3). P. 183–200. [https://doi:10.1023/A:1009995426001](https://doi.org/10.1023/A:1009995426001)

04.09.2023,  
29.09.2023